NEUTRON INDUCED CROSS SECTION DATA FOR IR-191 AND IR-193

YONG DEOK LEE* and YOUNG OUK LEE
Korea Atomic Energy Research Institute
150 Deokjin-dong, Yuseong-gu, Daejeon 305-353, Korea
*Corresponding author. E-mail : ydlee@kaeri.re.kr

Received May 23, 2006
Accepted for Publication August 1, 2006

The neutron induced nuclear cross section data for Ir-191 and Ir-193 were calculated and evaluated from unresolved resonance energy to 20MeV. The energy-dependent optical model potential parameters were determined based on the experimental data and applied up to 20MeV. A spherical optical model, a statistical model in an equilibrium energy region, and a multistep direct and multistep compound model in a pre-equilibrium energy region were used in the calculations. The direct capture model enhanced the fast neutron capture in the pre-equilibrium energy. The theoretically calculated cross sections were compared with the experimental data and the evaluated files. The calculations were found to be in good agreement with the experiment data. The evaluated cross section results were compiled with the ENDF-6 format. The fast energy results will be merged with the resonance parts to create a full evaluation library. The improvement of the neutron-induced cross section data will contribute to an increase in the efficiency of the production of Ir-192 as a radiation source.

KEYWORDS : Neutron, Cross Section, Evaluation, Data Library, Radiation Source

1. INTRODUCTION

The neutron cross section calculations and evaluation results are presented for Ir-191 and Ir-193 from several keV up to 20 MeV for the (n, tot), (n, n), (n, n'), (n, γ), (n, p), (n, a), (n, 2n) and (n, 3n) reactions. Iridium emits intense gamma rays in particular, Ir-192 is a major gamma ray source material and is widely used in several areas, for example material assays, non-destructive testing and in medical treatments. For the purpose of the above utilizations, Ir-192 is mainly produced in an isotopic production nuclear reactor by the neutron capture process of Ir-191. Using a threshold reaction with a high neutron energy, Ir-192 can be produced from Ir-194 through the process of neutron capture and decay. Ir-192 has a half-life of 73.82 days at a ground state . The half-life life at the 56.7keV first meta-state is 1.45 minutes while it is 241 years at the 168 keV meta-state. Ir-192 has a beta decay that produces Pt-192 and an electron capture that produces Os-192. The major emitted gamma rays from Ir-192 are 604keV, 316keV and 468keV from a ground state decay.

Ir-191 and Ir-193 exist at 37.3% and 62.7%, respectively, in their natural states . Ir-191 and 193 are stable isotopes. In a fission reactor, Ir-191 is produced from Os-191 through beta decay and Pt-191 by an electron capture. Ir-191 has 0.171MeV and 2.047MeV excited states with 4.94 and 5.5 seconds of a half-life, respectively. Ir-193 can be produced from the beta decay of Os-192 and the electron capture of Pt-193.

ENDF/B-VI has a fairly recent evaluation of Ir-191 and Ir-193; they were evaluated in 1995 and this was distributed in 1997(by R.Q. Wright, ORNL) [1]. For Ir-191, the total cross section was modified from 10 to 130keV. The total is 19% higher than that of natural iridium at 10keV, while it was unchanged above 130keV. From 2 to 20MeV, the capture data were obtained by the renormalization of the natural iridium capture to the Macklin data of Ir-191 at 2MeV of energy. For Ir-193, the total cross section was modified from 10 to 150keV. The total is 17% higher than that of natural iridium at 10 keV and unchanged above 150keV. For Ir-191 and –193, ENDF/B-VI has (n, 2n), (n, 3n), (n, p) and (n, a) cross section data identical to the BROND natural iridium evaluation. The recently evaluated ENDF/B-VII file adopted the cross section data from ENDF /B-VI release 8 for Ir-191 and Ir-193. The JEFF3.1 file adopted the ENDF/B-VI.8 data. However, the JENDL file does not include the cross section data for the iridium isotopes.

The Scat2-Empire code [2] combination was adopted in the current cross section calculation for the total, elastic scattering and threshold reaction cross sections. The evaluation consists of an optical model calculation followed by a complete nuclear reaction model calculation. The energy dependent optical model potential was applied for the

calculation of the transmission coefficients. The discrete and continuum energy levels were decided for all of the compound and residual nuclei.

The calculated cross sections were graphically compared with the experimental data and the evaluated file(ENDF /B-VI). The results were compiled as the ENDF-6 format. A general information file(MF1) was setup for each nucleus, including an evaluation history, code utilization, nuclear models used, evaluation procedure, tuning parameters, resonance description, reaction description and references. The evaluation in the fast energy region will be merged with the resonance part in the future.

2. NUCLEAR MODELS

2.1 Optical Model

The optical model is used in a transmission coefficient calculation to provide the total, elastic scattering and reaction cross sections for the target nucleus. In this case, the potential in the optical mode plays an important role in the coefficient calculation. From the relationship between the potential function and the incident particle energy, the solution of Schroedinger's equation finally calculates the cross sections.

Generally, the potential in the optical model is composed of several different parts. The total potential function is defined as

$$U(r,E) = V(r,E) - iW_V(r,E) - iW_D(r,E) + V_{so}(r,E) + V_c,$$

where $V(r, E)$ is the real volume potential, $W_v(r, E)$ is the imaginary volume potential, $W_D(r, E)$ is the imaginary surface potential, $V_{so}(r, E)$ is the spin-orbit interaction potential and $V_c(r, E)$ is the coulomb potential. Each potential type has its own form factor, as:

$$V(r,E) = V(E) f(r,R_V,a_V)$$
$$W_V(r,E) = W_V(E) f(r,R_V,a_V)$$
$$W_D(r,E) = W_D(E) \frac{d}{dr} f(r,R_V,a_V)$$
$$V_{so}(r,E) = V_{so}(E) \frac{1}{r}\frac{d}{dr} f(r,R_V,a_V)$$
$$V_c(r) = \frac{Zze^2}{2R_c}.$$

The form factor f is a function of the radius r and diffuseness a. A widely known form factor is a Woods-Saxon shape. The Woods-Saxon shape is well introduced in each potential type. The real part potential used in an optical model is

$$V(r) = -V/(1+\exp((r-R_v)/a_v)) \quad (1)$$

where V and a_v are the strength and diffuseness, respectively, of the potential. The nuclear radius R_v, related to the mass number A, is given by

$$R_v = r_v A^{1/3}. \quad (2)$$

The potential parameters were searched based on the reference experimental data. For the imaginary part potential, a derivative of the Woods-Saxon shape is used.

$$W(r) = -4W\exp((r-R_w)/a_w) / (1+ \exp((r-R_w)/a_w)^2 \quad (3)$$

Here, W, R_w and a_w are the potential strength, radius and diffuseness, respectively. Generally, the Thomas form is used in the optical model potential for a spin-orbit coupling:

$$V_{s\text{-}o}(r) = (2\,\overline{L} \bullet \overline{S})V_{so}(2/r)\{d/dr(1/[1+\exp((r-R_{so})/a_{so})])\} \quad (4)$$

In this equation, $\overline{L} \bullet \overline{S}$ is the dot product of the orbital and spin angular momentum operator.

The potential parameters in the optical model are expanded as a function of the incident neutron energy to describe an improved calculation for the energy dependent experimental data. The strength and radius of the real and imaginary parts were expanded as:

$$V = V_o + V_1 E_n, \quad r_v = r_{vo} + r_{v1} E_n \quad (5a)$$

$$W = W_o + W_1 E_n, \quad r_w = r_{wo} + r_{w1} E_n \quad (5b)$$

where E_n is an incident neutron energy. Thirteen potential parameters (V_o, V_1, r_{vo}, r_{v1}, a_v, W_o, W_1, r_{wo}, r_{w1}, a_w, V_{so}, r_{so}, a_{so}) were searched simultaneously in the optical model code. Table 1 shows the searched parameters based on the measurement data for the natural element.

2.2 Reaction Model

Empire is a modular code system. The main utilities include the masses, level densities and the discrete levels, the decay schemes, deformation parameters, γ-ray strength functions, RIPL, ENDF-6 formatting and the plotting capabilities. The main modules are: the Optical model, Multi-

Table 1. The Selected Energy-dependent Optical Model Potential Parameters: 1keV~20MeV Incident Neutron Energy Range

Parameter	Ir
V_o(MeV)	47.0100
V_1(MeV)	-0.267
r_{vo}(fm)	1.2668
a_v(fm)	0.66
W_o(MeV)	9.520
r_{wo}(fm)	1.2403
a_w(fm)	0.480
V_{so}(MeV)	7.000
r_{so}(fm)	1.2668
a_{so}(fm)	0.660
W_1(MeV)	-0.053
rw_1(fm)	0.000
rv_1(fm)	0.000

Table 2. Reference Experimental Data and 1st Excited Energy

Isotope	(n, γ) cross section	1st excited energy(keV)
Ir-191	1978Macklin, 1976Lindner	82
Ir-193	1978Macklin, 1994Koehler	73

step Direct(MSD) and Compound(MSC), Pre-equilibrium exiton model(DEGAS) and Monte Carlo hybrid simulation (HMS) and a full featured Hauser-Feshbach including the width fluctuation correction.

The individual nuclear reaction cross sections are calculated using the Hauser-Feshbach model for the equilibrium energy region. The emissions of neutrons, protons, a-particles and a light ion are taken into account along with the competing fission channel. In the statistical model of nuclear reactions, the Compound Nucleus(CN) state a with a spin J, parity π and excitation energy E to a channel b is given by the ratio of the channel width Γ_b to the total width $\Gamma_{tot} = \Sigma_c \Gamma_c$ multiplied by the population of this state $\sigma_a(E, J, \pi)$. This also holds for secondary compound nuclei that are formed due to the subsequent emissions of the particles. Each such state contributes to the cross section.

$$\sigma_b(E,J,\pi) = \sigma_a(E,J,\pi)\frac{\Gamma_b(E,J,\pi)}{\sum_c \Gamma_c(E,J,\pi)} \qquad (6)$$

These must be summed over the spin J and parity π and integrated over an excitation energy E(in case of the daughter CN) to obtain observable cross sections. Table 2 shows the reference experimental data and the 1st excited energy for the reaction calculation in the Empire.

The quantum mechanical approach for the calculation of the pre-equilibrium energy region is used. In the MSD approach, a continuum scattering is considered as a sequence of 1p-1h transitions and the transition strength functions correspond to the response functions of an external one-body operator acting repeatedly on a nucleus. The approach to a statistical multistep direct reaction is based on the MSD theory of a pre-equilibrium scattering for the continuum originally proposed by Tamura, Udagawa and Lenske [2]. The direct capture model [2] was inserted to enhance the fast neutron capture cross section in the pre-equilibrium energy range. The modeling of the MSC processes follows the approach of Nishioka et al. (NVWY) [2]. Similar to most pre-compound models, the NVWY theory describes the equilibration of the composite nucleus as a series of transitions along a chain of classes of closed channels of increasing complexity.

2.3 Level Density

The dynamic approach to the level densities is considered in the Empire. This takes into account the collective enhancements of the level densities due to the nuclear vibration and rotation. The level density is corrected for the rotational and vibrational collective effects in the non-adiabatic mode. In the case of the oblate nuclei, which are assumed to rotate parallel to the symmetry axis, the equation is given as

$$\rho(E,J,\pi) = \frac{1}{16\sqrt{6\pi}}\left(\frac{\eta^2}{\Im_{\parallel}}\right)^{1/2} a^{1/4} \sum_{K=-J}^{J} \left(U - \frac{\eta^2[J(J+1)-K^2]}{2\,|\,\Im_{eff}\,|}\right)^{-5/4} \exp\left\{2\left[a\left(u - \frac{\eta^2[J(J+1)-K^2]}{2\,|\,\Im_{eff}\,|}\right)\right]^{1/2}\right\}. \qquad (7)$$

Here, a is a level density parameter, J is the nucleus spin and K its projection, E is the excitation energy, U is the excitation energy less pairing (Δ), $\Im_{eff}$ is the effective moment of inertia and $\Im_{eff}$ is the parallel component. This equation includes a summation over the projection of the angular momentum K and thus it automatically accounts for the rotational enhancement. This equation accounts also for the vibrational enhancement, which is less important, by multiplying K_{vib} in the equation.

$$K_{vib} = \exp\left\{1.7\left(\frac{3m_0A}{4\pi\hbar^2 S_{drop}}\right)^{2/3} T^{4/3}\right\}. \qquad (8)$$

where $S_{drop} = 17/4\pi r_0^2$ and $r_0 = 1.26$. T is a nuclear temperature.

3. EVALUATION PROCEDURE

As a preliminary step, the available experimental data and the evaluated files(ENDF/B-VI, JENDL-3, JEF-2, BROND-2 and CENDL-2) in the required energy range were retrieved and analyzed. The optical model potential shape and the corresponding parameters, based on the total and elastic scattering experimental data, were sought, and the determined potential is applied for the calculation of the total, elastic scattering and reaction cross sections data as well as the transmission coefficients for a further reaction cross section calculation.

Using the obtained data, Empire calculates the individual reaction cross sections. The calculated cross sections are formatted as ENDF-6 and the calculation is compared graphically with the experimental data and the evaluated files using Zvview [2], which is a graphic interface package attached to Empire. If the result is satisfactory in the energy range of interest, the results are combined with the resonance part to make a full data library. If not, the evaluation undergoes a tuning process [3]. The final formatted file undergoes physics checking using CHECKR, FIZCON and PSYCHE codes [4].

4. RESULTS AND DISCUSSIONS

Ir-191 and Ir-193 do not have experimental data for the total cross section. Therefore, the total experimental data [5] for a natural element was used instead in the fast energy region for the optical model potential parameter search. In ENDF/B-VI, the total cross section was modified from 10 to 130keV, and it was 19% higher than that of natural iridium at 10keV. In this paper, several reaction cross sections are presented.

Fig. 1 shows a comparison of the calculated total cross section with the experimental data and the evaluated files for Ir-191 and Ir-193. The determined potential parameters for the natural element were used for Ir-191 and Ir-193. The calculation is in good agreement with the experimental data [5] and ENDF/B-VI. However, from 100keV to 500 keV, the calculation is ~5% higher than the measured data [1965 Tabony]. In this energy range, a normalization process to the experimental data was completed, and consistency was considered. The elastic cross section was modified to maintain consistency; however, any further changes of the potential parameters will influence the change of the calculated total cross section in the fast energy region. Above 1 MeV, the calculation is in good agreement with the measured data and ENDF/B-VI.

Fig. 2 shows the capture cross section for Ir-191. This evaluation is based on the Macklin experimental data [6]. The evaluated data show good agreement with the experimental data and the current ENDF/B-VI. However, at the higher energy region above ~ 3MeV, the calculation begins to deviate from ENDF/B-VI. In particular, above 10MeV, which is the pre-equilibrium energy region, the calculation shows a direct capture feature. Conversely, the ENDF/B-VI decreases continuously in that energy region.

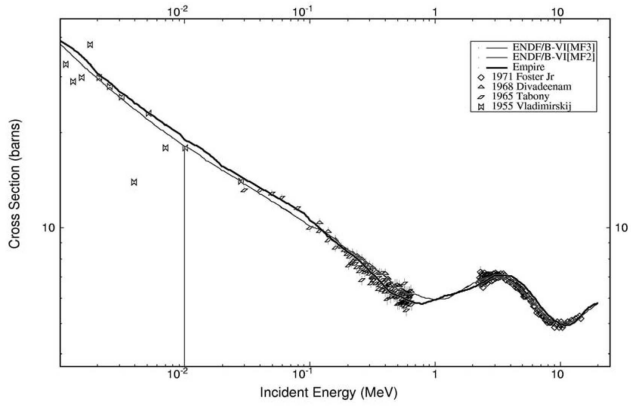

Fig. 1. (n, tot) Cross Section of Ir-191 and Ir-193 (The experimental data shown in the figure are from the natural iridium element)

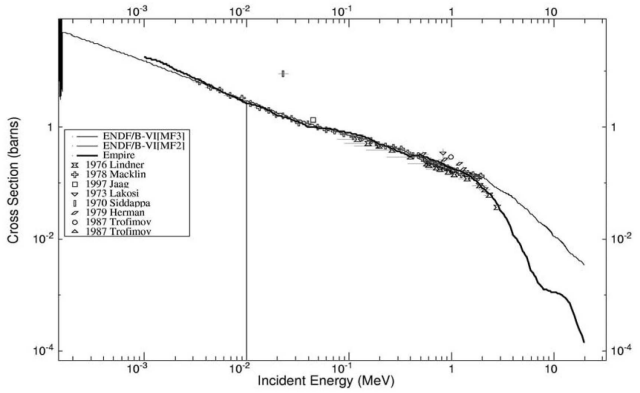

Fig. 2. (n, γ) Cross Section of Ir-191

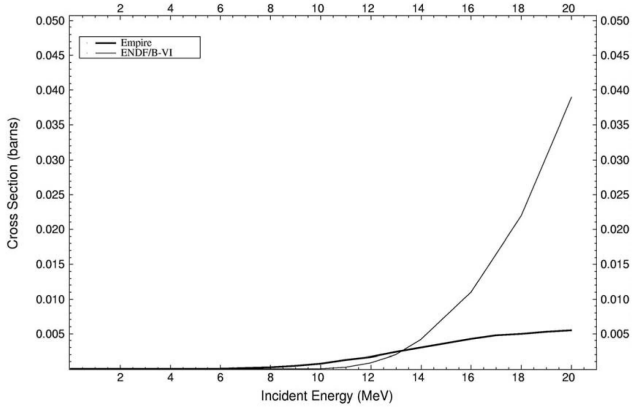

Fig. 3. (n, p) Cross Section of Ir-191

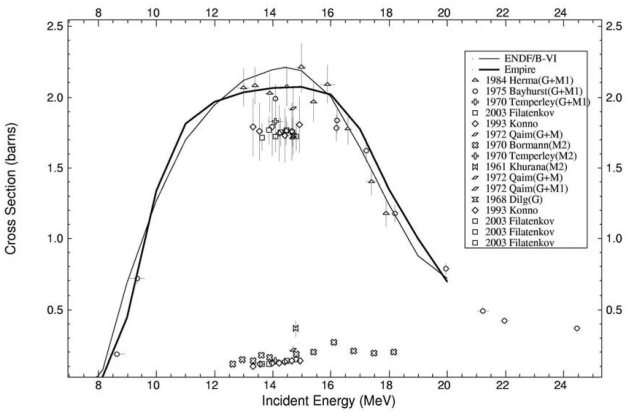

Fig. 4. (n, 2n) Cross Section of Ir-191

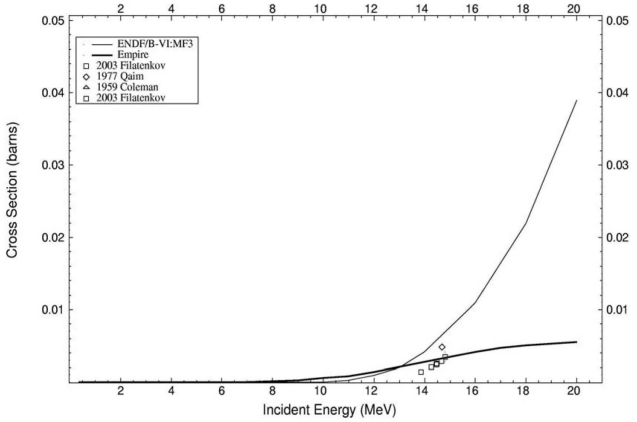

Fig. 7. (n, p) Cross Section of I-193

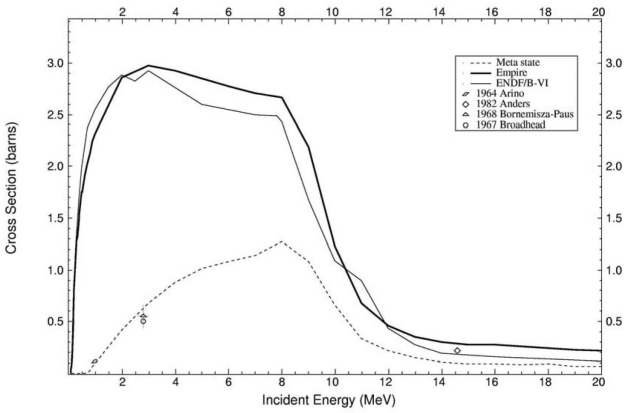

Fig. 5. (n, n') Cross Section of Ir-191

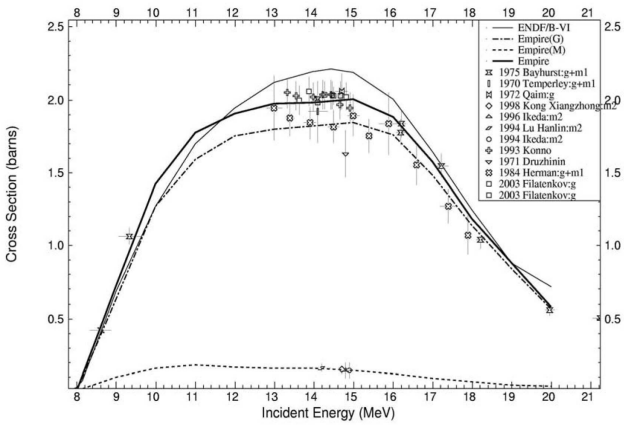

Fig. 8. (n, 2n) Cross Section of Ir-193

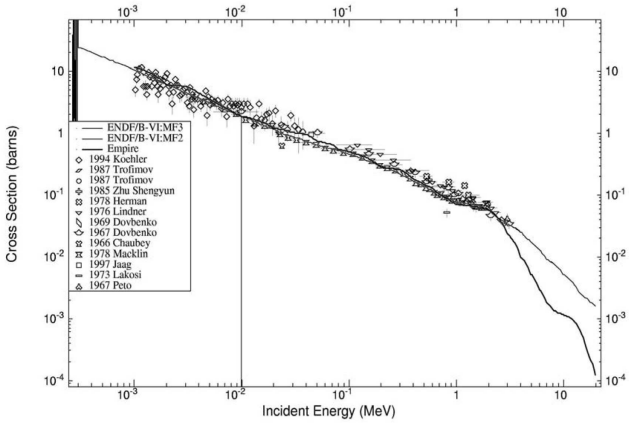

Fig. 6. (n, γ) Cross Section of I-193

Fig. 3 shows the neutron-induced proton production cross section. ENDF/B-VI shows a sharp increase, but the calculation shows a very smooth increase with the combination of the (n, np) channel open. Fig. 4 shows the (n, 2n) cross section for Ir-191. There is much measured data for the ground and meta-state decay. In addition, each data point has a different value due to error fluctuation. The calculation and ENDF/B-VI are in good agreement with the experimental data [7] within the fluctuation. However, around 14MeV, the calculation is slightly lower, by ~7%, compared to that of ENDF/B-VI. Fig. 5 shows the inelastic scattering cross section of Ir-191. Here, the experimental data [8,9] are only for the meta-state case. However, the calculation is in good agreement with the measured data [8] at 2.8MeV while the calculation for the meta-state is lower than that of the experimental data [9] at 14.6NeV.

Fig. 6 shows the capture cross section for Ir-193. The calculation and ENDF/B-VI agree well with the experimental data [6,10] in the measured energy region. The difference between the calculation and ENDF/B-VI starts at 3MeV. The calculation shows an improved shape in the pre-equilibrium region above 10MeV. Fig. 7 shows

the (n, p) cross section for Ir-193. The calculation follows the measured data [11] at around 14.5MeV. The shapes between the calculation and ENDF/B-VI differ somewhat.

Fig. 8 shows the (n, 2n) production cross section for Ir-193. The (n, 2n) cross section is another threshold process after the neutron capture to produce Ir-192. As shown in the figure, this reaction occurs mainly at a fast neutron incident. There are several measured data [12,13,14,15] for the ground state and meta-state decay. The calculation for the meta-state is in good agreement with the measured data [12]. The fluctuation between the measured data is somewhat large. ENDF/B-VI shows a higher result, at ~10 %, compared to the calculation at 14.5MeV. The calculation for the ground state decay is in good agreement with the Herman measured data [13]. The calculation is in good agreement with the sum of the measured data from the ground and meta-state decay [14].

5. CONCLUSIONS

Neutron induced reaction cross sections for selected iridium isotopes were successfully evaluated in the fast energy region. The capture and other threshold calculated cross sections were in good agreement with the experimental data. Including the meta-state measured data, the calculations for the threshold reaction cross sections showed good agreement. A good example is the (n, 2n) reaction. At the pre-equilibrium energy region, the calculated capture cross section showed the fast neutron direct capture phenomena. For the production of Ir-192, an improvement of the neutron capture cross section of Ir-191 and the (n, 2n) threshold cross section of Ir-193 is required to increase the production efficiency. However, the production of Ir-192 from Ir-193 needs a high energy neutron due to the threshold reaction. Therefore, in a thermal nuclear reactor, the capture cross section of Ir-191 is more important.

At the 168 keV meta-state of Ir-192, it has a long half-life, at 241 years. However, the gamma contribution at that state is very small in the total capture gamma production, at less than 0.1%. However, due to the long half-life, careful management is considered for storage sites. The evaluated results were converted into the ENDF-6 format.

ACKNOWLEDGEMENT

This work was performed under the auspices of the Korea Ministry of Science and Technology as a long-term R&D project.

REFERENCES

[1] ENDF/B-VI, Brookhaven National Laboratory, Upton, NY, 2000.
[2] M. Herman, P. Oblozinsky, R. Capote, M. Sin, A. Trkov, A. Ventura and V. Zerkin. Recent Developments of the Nuclear Reaction Model Code EMPIRE, in the Proceedings of the International Conference on Nuclear Data for Science and Technology, published in AIP Conf. Proc. Vol. 769, p.1184, ISBN 0-7354-0254-X, 2005.
[3] Y.D. Lee and J.h. Chang, "Neutron Cross Section Data Library for Pd-105, Ag-109, Xe-131 and Cs-133," J. of KNS, vol.37 no. 1, p. 101, 2005.
[4] IAEA Nuclear Data Center, www-nds.iaea.org, 2006.
[5] D.G. Foster JR, D.W. Glasgow, "Neutron Total Cross Sections, 2.5 - 15MeV," J, PR/C, 3, 576, 1971.
[6] L. Macklin, D. Drake and J. Malanify, "Fast Neutron Capture Cross Section of Tm-169, Ir-191, Ir-193 and Lu-175 for Neutron Energy between 3 and 2000keV," R, LA-7479-MS, 1978.
[7] M. Herman, A. Marcinkowski, K. Stankiewicz, "Cross Sections for (N,2N) Reaction on Ir-191 and Ir-193, J, JP/G, 10, 91, 1984.
[8] P. Bornemisza-Pauspertl et al., "Measurements on the Excitation Cross Sections of Isomeric States by Scattering of 2.8MeV Neutrons," J, AK, 10, (2), 112, 1968.
[9] B. Anders, R.Pepelnik, H.-U.Fanger, "Application of a Novel 14MeV Neutron Activation Analysis System for Cross Section Measurements with Short-Lived Nuclides," C, 82ANTWER, 859, 1982.
[10] P. E. Koehler and F. Kappeler, "Measurements of (n,g) Cross Sections for Very Small Stable and Radioactive Samples of Interest to the s- and p-Process," C, 94GATLIN, 179, 1994.
[11] A. A. Filatenkov, S. V. Chuvaev, "Experimental Determination of Cross Sections of a Set of Badly Known Neutron Induced Reactions for Heavy Elements (Z=74-79)," R, RI-259, 2003.
[12] Kong Xiangzhong et al., "Activation Cross Sections for Generation of Long-Lived Radionuclides," J, JRN, 227, 15, 1998.
[13] M. Herman, A. Marcinkowski, K. Stankiewicz, "Cross Sections for (N,2N) Reaction on IR-191 and IR-193," J, NP /A, 430, 69, 1984.
[14] C. Konno et al., "Activation Cross Section Measurement at Neutron Energy from 13.3 to 14.9MeV," R, JAERI-1329, 1993.
[15] S.M. Qaim, "Activation Cross Sections, Isomeric Cross Section Ratios and Systematics of (n,2n) Reactions at 14-15MeV," J, NP/A, 185, 614, 1972.